Spectroscopically and Spatially Resolving the Components of Close Binary Stars
ASP Conference Series, Vol. 318, 2004
R. W. Hilditch, H. Hensberge, and K. Pavlovski (eds.)

Improvement of Spectroscopic Binary Star Orbits Through the Use of Spectral Disentangling

David E. Holmgren

SMART Technologies, Inc., Bay 8, 1420 28 Street N.W., Calgary, Alberta, T2T 6G1, Canada

Abstract. A review of orbit improvement for spectroscopic and eclipsing binary stars is presented. Specifically, capabilities for orbital and line profile analyses of these systems using the KOREL disentangling program (Hadrava 1995; 1997) are discussed. After a short literature review, criteria and possible paths for orbital improvement are presented, namely a procedure for including visual data in a disentangling solution, along with possible optimization algorithms. A solution "template", based on the study of V578 Mon by Hensberge et al. (2000), is presented. Analyses of specific systems are presented, showing explicitly how disentangling has resulted in improved orbits and a better general understanding of each system. Comparisons with more traditional methods such as cross - correlation are made for this purpose.

1. Introduction

Disentangling of the optical wavelength range spectra of spectroscopic and eclipsing binary star systems is a powerful tool for advancing our knowledge of stellar dimensions and hence stellar evolution. The intent of this review is to provide a sense of what can be attained through the careful use of disentangling.

One can view disentangling as the logical extension of cross - correlation (CCF hereafter) radial velocity measurement (Simkin 1974, Hill 1982) and tomographic spectral separation (Baguolo & Gies 1991). The two-dimensional CCF measurement (Zucker & Mazeh 1994) and broadening function (Rucinski 1992) techniques should also be recalled in this context.

Disentangling represents a *significant* advance because both radial velocity (RV hereafter) measurement and orbit computation are handled together in a self - consistent manner; they are no longer separate, distinct operations. The technique also allows one to take full advantage of the information present in digital spectra, with the high dynamic range of modern solid-state sensors allowing the detection of very weak signals, such as the spectrum of a faint secondary star. This is of particular importance in studies of binary systems in nearby galaxies.

The present review will be limited to a discussion of early-type binary systems, as it is to these systems which spectral disentangling has largely been applied. Following a short literature review in the next section, paths to orbit improvement will be discussed, along with a solution "template" for disentangling. Finally, analyses of specific systems (β Sco A and AR Cas) will be presented to demonstrate what can be attained with disentangling, and to compare this technique to more traditional methods of RV measurement and orbital solution.

2. Disentangling - a literature review

A technical review of spectral disentangling is presented by Hadrava (2004, this volume), although the original papers by both Hadrava (1995; 1997) and Simon & Sturm (1994) should be consulted, especially for implementation details and extensions.

It is worth making the distinction between the Fourier domain approach used by Hadrava, and the wavelength domain method of Simon and Sturm. As Hadrava notes in his review in this volume, the two approaches are entirely equivalent; one can think in this respect of the momentum and position representations used in quantum theory. The great advantage of the Fourier domain approach is that it makes the application of disentangling much more tractable; the matrices involved in computing the solution are of the order of the number of stars in the system being analyzed as opposed to the number of data points in a spectrum (which can be quite large). The latter requires sparse matrix and SVD techniques to be used in computing the solution, whereas KOREL requires only FFT and simplex optimization routines.

The underlying model in KOREL is one in which two single-star spectra are shifted in radial velocity to match the positions of the component spectra of a binary system at any particular orbital phase. This includes implicitly the light ratio at the corresponding wavelength. In the frequency domain, this velocity shifting results, via the convolution theorem, in a linear set of equations for the Fourier components of the individual component spectra. Solving these equations at each frequency allows the Fourier transform of each component spectrum to be built up. The orbit is then recovered by optimizing this calculation over the orbital elements. An inverse FFT at the end of the optimization produces the component spectra, which can then be cross-correlated with the blended spectra to produce a set of RVs.

To date, spectral disentangling has played a role in the analyses of over 16 binary systems, most of them of early spectral type. Table 1 summarizes these in chronological order. What is interesting to note about these is that many of the studies are of binary systems either in star clusters (e.g., V578 Mon, V497 Cep) or in nearby galaxies (e.g., HV 982). Also, much of the work has been done using Hadrava's KOREL code. Many workers are clearly pushing the capabilities of KOREL in applying it to these relatively faint systems.

3. Paths to orbit improvement

The combination of RV measurement and orbit calculation in disentangling allows for a self-consistent analysis of a system. But how can one measure orbit "improvement"? Some possibilities are: computing the RMS error of fit and the covariance matrix, determining the errors in the RVs, consideration of the phase coverage of the data, and the quality of the spectra themselves (i.e., signal-to-noise ratio). As disentangling effectively side-steps radial velocity measurement, finding the errors in the RVs themselves is no longer a consideration. The RMS error of the fit, often taken to be the RV error itself ($\pm\sigma_1$ in km s^{-1}), involves certain assumptions (e.g., normality of the fit residuals) which may or may not be met with a given data set. With disentangling, what matters more is phase

Table 1. Binary system studies using spectral disentangling techniques.

System	Reference
V453 Cyg	Simon & Sturm (1994)
Y Cyg	Simon et al. (1994)
β Cep	Hadrava & Harmanec (1996)
V436 Per	Harmanec et al. (1997)
β Sco A	Holmgren et al. (1997)
AR Aur	Zverko et al. (1997)
SZ Cam	Lorenz et al. (1998)
V606 Cen	Lorenz et al. (1999)
AR Cas	Holmgren et al. (1999)
η Lyr A	Bisikalo et al. (2000)
V578 Mon	Pavlovski & Hensberge (2000)
V578 Mon	Hensberge et al. (2000)
HV 982	FitzPatrick et al. (2002)
EROS 1044	Ribas et al. (2002)
o Leo	Griffin (2002)
SMC binaries	Harries et al. (2003)
HV 5936	FitzPatrick et al. (2003)
V497 Cep	Yakut et al. (2003)
V436 Per	Janík et al. (2003)

coverage and data quality. If one thinks in particular of the reconstruction of the component spectra, it should be clear that spectra well-distributed over all orbital phases are required in order to sample all of the Doppler shift "bins" necessary to completely recover a line profile. Of course, adequate phase coverage is also necessary to recover the shape of the RV curve. Examples of just what is meant by sufficient phase coverage will be illustrated later through examples.

However, to get the most out of disentangling, it is necessary to incorporate all possible sources of data. This in turn points toward certain extensions of the method.

3.1. Using visual data

The KOREL program can be used for the analysis of multiple systems and in some cases, visual data may be available. These can take the form of position angle and separation pairs (ρ, θ), or visibilities obtained from optical, infra-red, speckle, and occultation interferometry. The visual data can then be viewed as "constraints" on the disentangling solution. More to the point, the disentangling and visual solutions can be combined directly, leading to something very similar to the visual-spectroscopic orbit problem discussed by Morbey (1975). Since KOREL minimizes a sum of squares S directly (involving the Fourier components, as discussed above), the visual data can be included by extending the sum of squares as (using position angle and separation as an example):

$$S = S_{spectra} + \sum \Big[\frac{\Delta_\theta}{\sigma_\theta}\Big]^2 + \sum \Big[\frac{\Delta_\rho}{\sigma_\rho}\Big]^2$$

where $\Delta_{\theta,\rho}$ denote fit residuals, and $\sigma_{\theta,\rho}$ denote measurement errors. An issue here is the correct relative weighting of the terms from the spectra and from the visual data, but this could also be handled by a penalty barrier method (Gill et al. 1981) in which the latter is given an arbitary weight which is changed systematically to find the limiting solution, i.e.,

$$\lim_{\alpha\to\infty} S_{spectra} + \alpha S_{visual}$$

In any case, the minimization would now include the usual visual orbit parameters $a, e, i, \omega, \Omega, T, P$ (semi-major axis in arcsec, eccentricity, inclination, longitude of periastron, longitude of the ascending node, time of periastron passage, and orbital period). After converging such a solution, computation of the system parallax is straightforward.

3.2. Optimization

At present, KOREL uses the simplex method (a multi-dimensional "amoeba", Press et al. 1992) to compute a solution. However, it may be desirable to use derivative - based methods, even for refining the solution. This would add some complexity as numerical derivatives with respect to the orbital elements would be required. What might be more effective in this case would be the variable metric algorithm, in which estimates of the gradient and inverse Hessian H^{-1} (i.e., the inverse of the least-squares normal equations matrix) of S are updated iteratively. An advantage of this technique is that it is possible to start with a poor initial estimate of H^{-1} and still converge. Of course, the inverse Hessian at the solution is directly related to the covariance matrix.

An alternative estimation model that could be used is the Gauss-Helmert one, in which both the model parameters and data are adjusted. This is the rigorously correct approach for nonlinear least-squares problems in several variables. It is described by Jefferys (1980, 1981) and also by Eichhorn & Xu (1990) in the context of visual binary orbits. If this approach were to be used, it would likely result in a more realistic covariance matrix.

4. A solution template

The study of the system V578 Mon by Hensberge et al. (2000, Fig. 1) provides a framework for obtaining a self-consistent model of a binary system, by correctly accounting for the "feedback" between different sources of data. However, for a given binary system, not all sources of data may be present (e.g., there may be no light curve). Here, a generalization of this approach is proposed. Given that visual data (position angles and separations, or interferometer visibilities) may be available, especially if the system is a multiple one, these could be integrated into the framework. Once the "feedback loop" is stabilized, then one could go on to compute covariance matrices, system dereddening, component magnitudes and so forth. Figure 1 illustrates this. Even if the visual data were not integrated directly into the disentangling, a separate program for analysing visual data and/or light curves could be used to generate the appropriate feedback mechanism.

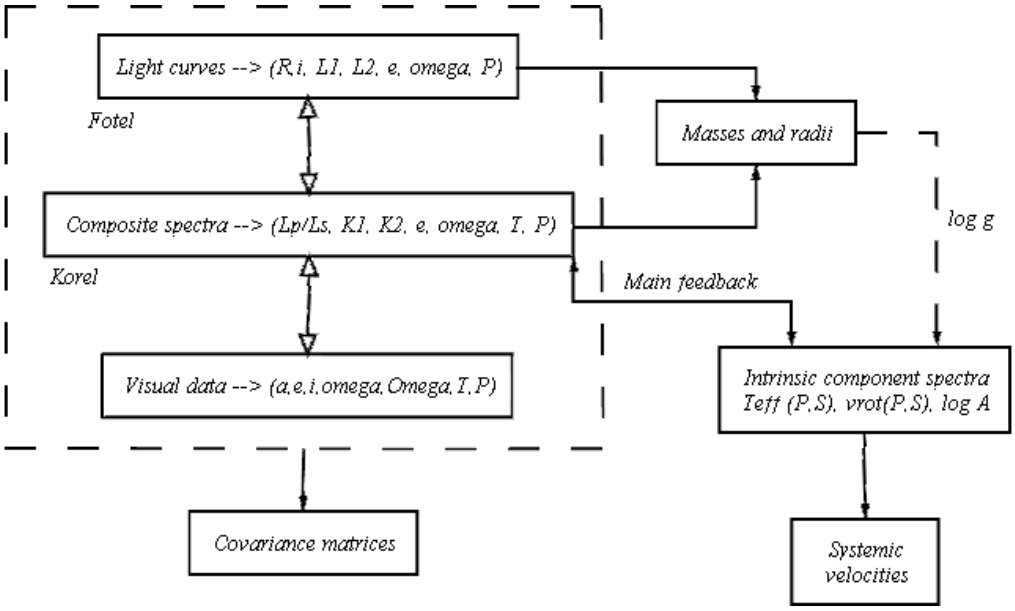

Figure 1. The interaction between results produced by disentangling (KOREL) and other sources of data.

5. Examples of disentangling

The systems to be reviewed here are β Sco A (Holmgren et al. 1997) and AR Cas (Holmgren et al. 1999). These give an indication of what can be attained with disentangling under different circumstances.

5.1. β Sco A

This is an example of a system for which we have virtually complete information. The orbit in three dimensions is available, as visual data from occultation interferometry are available. This of course allows the parallax and distance to be computed. Disentangling of the line profiles leads to the spectroscopic orbit, radiative parameters, and rotational velocities. From all of this, the absolute dimensions are found. Also, a measurable apsidal motion allows a mean internal structure constant (ISC) for each component to be found, hence providing additional constraints on their evolutionary states.

The spectral data available consisted of 26 Reticon spectra at Hα, obtained using the Ondřejov 2m telescope, and some 600 historical RVs found in the literature. The latter were important in deriving a precise apsidal motion rate. The KOREL disentangling solutions for He I 667.8 nm and Hα 656.3 nm were well-defined as the phase coverage was sufficient, and the signal-to-noise ratios of the spectra were all high. The telluric lines around Hα were treated as a "third component", whose orbit was known. The resulting component profiles (not corrected for the light ratio) and RVs are shown in Fig. 2. Line photometry

generated by KOREL (Hadrava 1997) indicated the possibility of an eclipse near one conjunction.

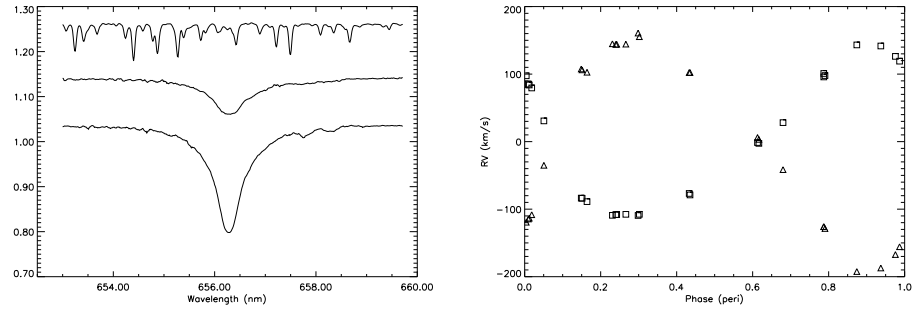

Figure 2. Disentangled Hα line profiles (left) for β Sco A: primary (bottom), secondary (middle), and telluric (top). The stellar profiles have not been corrected for the light ratio. The radial velocity curves are shown in the right panel.

The visual data consisted of two occultation (Moon and Jupiter) measurements which, when combined with the RVs from the disentangling solution, produced the system parallax. Here, the visual-spectroscopic orbit calculation of Morbey (1975) was used.

Cross-correlation RV measurements were also made using He I 667.8 nm, and it is interesting to compare the RMS errors of the orbit based on these data with those from KOREL. The latter produced $\pm$5.9 km s^{-1}, as compared to $\pm$7.8 km s^{-1} for the CCF data. The disentangling results are clearly an improvement over the CCF method. Similarly, the Hα KOREL solution produced an RMS error of $\pm$6.5 km s^{-1}. To put this further into context, a FOTEL solution for all available RV data (including zero-point offsets for different sources of data), gave $\pm$21 km s^{-1}. Clearly, the KOREL solutions helped produce more well-defined RV curves and hence a superior set of absolute dimensions.

5.2. AR Cas

This is a system well-known for presenting observational challenges; the orbital period is very close to 6 sidereal days, and a light ratio $\sim$ 40 has prevented direct detection of the secondary star. The extreme light ratio also presents a challenge for KOREL.

Spectral data were obtained with the Ondřejov 2m telescope and Reticon detector, and with the UBC 4096 CCD on both the 1.8m and 1.2m telescopes of the Dominion Astrophysical Observatory. All spectra were centered on Hα. Échelle spectra were obtained with the 2m telescope of the San Pedro Martir observatory. The wavelength range covered by these data was 369.6 nm to 760.0 nm. Good phase coverage required telescopes on two continents.

A new light curve was obtained as well, again requiring observations from sites at different longitudes (Hvar, San Pedro Martir, Tandogan, and Hipparchos). These data, as well as RVs available in the literature, were critical in refining the apsidal motion rate. The light curve analysis resulted in improved physical parameters (radii, temperatures) and light ratio.

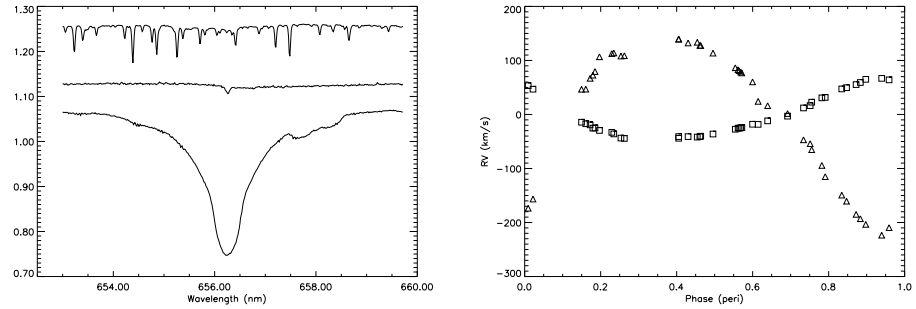

Figure 3. Disentangled Hα line profiles (left) for AR Cas: primary (bottom), secondary (middle), and telluric (top). The stellar profiles have not been corrected for the light ratio. The radial velocity curves are shown in the right panel.

The disentangled profiles and radial velocity curves are shown in Fig. 3. The primary spectrum is that of a B4V star, and it is worth pointing out here that KOREL has correctly reconstructed the C II lines near 658.0 nm. The secondary spectrum, that of an A6V star, was recovered using KOREL in both the red (Hα, complete solution) and blue (decomposition only, no orbital solution). That the solution gave a consistent result was checked using the blue data, specifically the strength of the secondary's Mg II 448.1 nm line. Model atmosphere spectra were used for this purpose.

As with β Sco A, the telluric lines around Hα were treated as a third component with variable line strengths and a known orbit.

A disentangling solution for He I 667.8 nm showed that this line is not present in the secondary star, thus confirming its spectral classification. Also, a set of difference spectra generated for this line indicated possible line profile variability.

In terms of the orbital solution, the RMS error of the fit found by KOREL was always smaller than that found through a conventional solution. CCF RV measurements of He I 667.8 nm and other published RVs were used as input for FOTEL, leading to a typical RMS error of ± 8.50 km s^{-1}. The corresponding RMS error from KOREL for this line was ± 6.03 km s^{-1}, demonstrating the better fit found by disentangling. For Hα, the RMS error for the primary was ± 1.93 km s^{-1}, and for the secondary ± 8.13 km s^{-1}. This shows that reliable results can be obtained even in the case of a large light ratio.

References

Bagnuolo, W. G., & Gies, D. R. ApJ, 376, 266

Bisikalo, D. V., Harmanec, P., Boyarchuk, A. A., Kuznetsov, O. A., & Hadrava, P. 2000, A&A, 353, 1009

Eichhorn, H. K., & Xu, Y.-L. 1990, ApJ, 358, 575

FitzPatrick, E. L., Ribas, I., Guinan, E. F., DeWarf, L. E., & Maloney, F. P. 2002, ApJ, 564, 260

FitzPatrick, E. L., Ribas, I., Guinan, E. F., Maloney, F. P., & Claret, A. 2003, ApJ, 587, 685

Gill, P. E., Murray, W., & Wright, M. H. 1981, Practical Optimization, (New York: Academic Press)

Griffin, E. M. 2002, AJ, 123, 988

Hadrava, P. 1995, A&AS, 114, 393

Hadrava, P. 1997, A&AS, 122, 581

Hadrava, P., & Harmanec, P. 1996, A&A, 315, L401

Harmanec, P., Hadrava, P., Yang, S., et al. 1997, A&A, 319, 867

Harries, T. J., Hilditch, R. W., & Howarth, I. D. 2003, MNRAS, 339, 157

Hensberge, H., Pavolvski, K., & Verschueren, W. 2000, A&A, 358, 553

Hill, G., 1982, Publ. Dominion Astrophys. Obs., 16, 59

Holmgren, D. E., Hadrava, P., Harmanec, P., Koubský, P., Kubát, J. 1997, A&A, 322, 565

Holmgren, D. E., Hadrava, P., Harmanec, P., et al. 1999, A&A, 345, 855

Janík, J., Harmanec, P., Lehmann, H., et al. 2003, A&A 408, 611

Jefferys, W. H. 1980, AJ, 85, 177

Jefferys, W. H. 1981, AJ, 86, 149

Lorenz, R., Mayer, P., & Drechsel, H. 1998, A&A, 332, 909

Lorenz, R., Mayer, P., & Drechsel, H. 1999, A&A, 345, 531

Morbey, C. 1975, PASP, 87, 689

Pavlovski, K., & Hensberge H. 2000, IAUS, 200, 109

Press, W. H., Teukolsky, S. A., Vetterling, W. T., & Flannery, B. P., 1992, Numerical Recipes, 2nd ed., (Cambridge: Cambridge University Press)

Ribas, I., FitzPatrick, E. L., Maloney, F. P., & Guinan, E. F. 2002, ApJ, 574, 771

Rucinski, S. M. 1992, AJ, 104, 1968

Simkin, S. 1974, A&A, 31, 129

Simon, K. P., & Sturm, E. 1994, A&A, 281, 286

Simon, K. P., Sturm, E., & Fiedler, A. 1994, A&A, 281, 286

Yakut, K., Tarasov, A. E., İbanoğlu, C., et al. 2003, A&A, 405, 1087

Zucker, S., & Mazeh, T., ApJ, 420, 806

Zverko, J., Žižňovský, J., & Khokhlova, V. 1997, Contr. Astron. Obs. Skalnaté Pleso 27, 41